ON THE USE OF HYBRID RANS/LES METHODS FOR THE SIMULATION OF THE EROSION OF A STRATIFIED LAYER BY A TURBULENT BUOYANT JET

F. Duval
Institut de Radioprotection et de Sûreté Nucléaire (IRSN)
Saint Paul-Lez-Durance, 13115, France
fabien.duval@irsn.fr

M. Le Bars
Aix-Marseille Université - CNRS, Ecole Centrale Marseille, I.R.P.H.E, UMR 7342
Technopôle Château-Gombert, 49 rue F. Joliot-Curie, 13384 Marseille cédex, France
lebars@irphe.univ-mrs.fr

ABSTRACT

This work deals with the ability of non-zonal hybrid RANS/LES methods to predict the erosion of a stable stratification by a turbulent buoyant jet. Such a situation may occur during a severe accident in a light-water-reactor. A hydrogen-rich mixture that has been accumulated in some area of the containment can be mixed by a free jet coming from a breach in the primary circuit. Different regimes characterizing the efficiency of the mixing have been identified experimentally according to the interfacial Froude number. Numerical results obtained an eddy-diffusivity RANS turbulence closure are presented in the frame of post-calculations of the OECD/NEA benchmark exercise addressing experiments conducted in the PANDA facility at the Paul Scherrer Institute. The obtained results along with other contributions to the benchmark exercise underline the difficulty to obtain accurate predictions for some regimes using RANS turbulence models and this argues to more sophisticated or alternate approaches. Among these, hybrid RANS/LES approaches appear to be a promising candidate for such large-scale simulations and transient durations as they try to retain the advantages of both RANS and LES approaches. Schematically, this consists in performing large eddy simulation on coarse grids using a RANS-like approach limited to the modeling of the subgrid scales. The proposed methodology is examined on small-scale experiments employing water and water-salt as simulants conducted at IRPHE. Such complementary experiments allow to gain access to the different regions of interest using non-intrusive measurement techniques and then enable a detailed comparison between the different approaches. A preliminary qualitative comparison clearly shows the potentialities of the hybrid approach.

KEYWORDS

Turbulence, stratified layer, erosion, hybrid RANS/LES simulation

1 INTRODUCTION

The development of hybrid methods RANS/LES for the simulation of turbulent flows has grown significantly since the last few years (*e.g* [10]). If such methods were initially developed in a zonal context to overcome a costly near-wall LES resolution, hybrid methods called continuous ensuring a seamless transition between RANS and LES resolution have known a growing interest. They allow to overcome the lack of universality of RANS methods by solving large vortices as in LES methods while maintaining the computational cost of RANS methods using relatively coarse meshes. Among the proposed methods, the SAS (Scale-Adaptive Simulation) [14, 13], PANS (Partially-Averaged Navier Stokes) [11, 12] and PITM (Partially Integrated Transportation Modelling) [16, 9] approaches are particularly attractive as they can be developed on the basis of a RANS subfilter closure model. As a result, they are expected to run as well as the used RANS model in the under-resolved regions of the flow while gaining accuracy (unsteady structures, anisotropy, ...) in some well-resolved other

regions. The potential for the aforementioned methods was illustrated on numerous wall-bounded constant-density turbulent flows and very promising results were obtained on relatively coarse meshes compared to well-resolved LES simulations.

On the other hand, the simulation of variable-density turbulent flows, due to thermal or compositional effects, using RANS/LES hybrid methods has received much less attention while the lack of universality of RANS models for such flow argues for the use of hybrid approaches. The situation of interest concerns here the mixing of a stable stratification by a turbulent jet. Such a situation may occur during a severe accident in a light-water reactor and corresponds to the mixing of hydrogen rich mixture that has been accumulated in some area of the containment by a free jet coming from a breach in the primary circuit. Depending on the efficiency of the turbulent mixing, the hydrogen may dilute or may ignite and then leading in this latter case to a pressure loading that can affect the integrity of the containment. Numerical studies recently performed in the frame of the OECD/NEA benchmark exercise addressing experiments conducted in the PANDA facility at the Paul Scherrer Institute have underlined the difficulty of eddy-diffusivity RANS turbulence models to predict accurately the erosion process [4]. As a result, this motivates for the use of alternate approaches, especially hybrid methodologies, as the use of LES appears to be somewhat prohibitive for such large-scale experiments and test duration.

The paper is organized as follows. After a brief review of the nondimensional parameters describing the mixing of a stable stratification and the different regimes observed, numerical results obtained in the frame of the OECD/NEA benchmark exercise using a k-ϵ RANS turbulence closure are presented. Then, a discussion on the interest of conducting complementary small-scale experiments is provided. The hybrid methodology is then presented and assessed on such small-scale experiments including a comparison with RANS and well-resolved LES simulations. Finally, first numerical results using the hybrid approach are presented in the frame of post-calculations of the benchmark exercise.

2 MIXING OF A STABLE STRATIFICATION

As stated in the introduction, the problem under statement corresponds to the mixing of a stable stratification by a turbulent jet. We will neglect here the effect of temperature and we will consider that the mixture behaves like a two-species mixture of perfect gases. Then, focusing first on the fluid injection, one can identify eight parameters. Those parameters are the injection diameter d_0, the injection velocity u_0, the gravity acceleration g, the mass diffusivity D, the densities ρ_h, ρ_l and the viscosities μ_h, μ_l of the heavy and light species respectively. These species correspond to the helium-rich mixture and air initially present in the vessel, we do not take into account in addition the physical properties of the injected mixture to simplify the analysis as the injected gas mixture is close to the (air) heavy species. As these parameters are expressed from three base units, namely mass [kg], space [m] and time [s], five independent dimensionless numbers describing the relevant physical phenomena are expected. The usual dimensionless numbers describing variable density turbulent jets are:

- The Reynolds number Re defined as the ratio of inertial forces to viscous forces. It is usually based on the injection characteristics and serves to characterize the turbulent flow:

$$\mathrm{Re} = \frac{\rho_0 u_0 d_0}{\mu_0}$$

  where ρ_0, μ_0 refer to the material properties of the injected fluid that are assumed to match the heavy species material properties ρ_h, μ_h.

- The Froude number Fr defined as the ratio of inertial forces to buoyancy forces. For buoyant jets, one usually adopt the densimetric Froude number [8] defined as:

$$\mathrm{Fr}^2 = \frac{\rho_0 u_0^2}{g d_0 (\rho_a - \rho_0)}$$

  Here again, ρ_0 refers to the material properties of the injected fluid whereas ρ_a refers to the ambiant fluid. Here, both ρ_0 and ρ_a match the heavy species density ρ_h.

- The Schmidt number Sc defined as the ratio of momentum diffusivity and mass diffusivity, expressed here from the light species properties:

$$\mathrm{Sc} = \frac{\mu_l}{\rho_l D}$$

- The density difference can be described through the Atwood number At that serves to characterize hydrodynamic instabilities for density stratified flows:

$$\mathrm{At} = \frac{\rho_h - \rho_l}{\rho_h + \rho_l}$$

- Finally, the viscosity difference is described through a reduced viscosity defined as:

$$\mathrm{R}_\mu = \frac{\mu_h}{\mu_l}$$

  For most cases of interest R_μ does not change significatively and is close to unity.

Using the numerical values from the benchmark specifications, one obtains the following set of dimensionless numbers: Re $\simeq 25400$, Fr $\simeq \infty$, Sc $\simeq 0.33$ and At $\simeq 0.19$. We just mention here that the values obtained for the Reynolds and the densimetric Froude number correspond to a turbulent pure (constant density) jet. In addition to the parameters defined above, one introduces the length h_s over which the mixture density changes linearly from ρ_h to ρ_l. As there is an additional parameter, there is also an additional independent dimensionless number describing the relevant physical phenomena. One usually adopts the interaction Froude number defined as:

$$\mathrm{Fr}_i = \frac{u_i}{\mathcal{N} d_i} \tag{1}$$

where $\mathcal{N}$ is the characteristic pulsation of the stratification called the Brunt-Väisälä frequency defined as:

$$\mathcal{N}^2 = -\frac{g}{\rho}\frac{d\rho(y)}{dy} \simeq \frac{2g}{\rho_h + \rho_l}\frac{\rho_h - \rho_l}{h_s} \tag{2}$$

The interaction Froude number is one of the most significant dimensionless number for buoyant jet interacting with a stratified layer as it allows to identify three distinct regimes. The first regime corresponds to the so-called diffusion regime for which buoyancy of the stratified layer dominates, $\mathrm{Fr}_i \ll 1$. On the other hand, when inertia dominates, $\mathrm{Fr}_i \gg 1$, the jet penetrates the whole stratification and this corresponds to the so-called dilution regime. The regime corresponding to intermediate values of the the interaction Froude number is called the erosion regime. In this case, the jet comes to interact with the density stratification but, as inertia is not sufficient to let the jet penetrates the stratified layer, the jet is redirected and comes to interact with the density gradient before moving downwards. The mixing takes place in this interaction region where the jet is redirected and is driven by both advection and molecular diffusion processes.
The impact velocity u_i of the jet and the jet diameter d_i at the stratified layer can be estimated from correlations giving the evolution of velocity and jet diameter along the jet centreline [6, 8]:

$$\frac{u(y)}{u_0} = B\frac{d_0}{y - h_0} \tag{3}$$

$$d(z) = C(y - h_0) \tag{4}$$

where B and C denote decay constants. Applying these correlations at the bottom of the stratified layer with $B = 6.2$ and $C = 0.172$ [8, 17] and using the numerical values from the benchmark specifications, one obtains $\mathrm{Fr}_i \simeq 1.88$. Hence, the expected regime corresponds here to the erosion regime. Such a regime involves two different characteristic time scales, namely a purely molecular diffusion time scale and a dilution-like one and constitutes the most difficult regime from a numerical modelling point of view [5, 18].

3 NUMERICAL RESULTS ON LARGE-SCALE EXPERIMENTS

In this section, numerical results obtained in the frame of the OECD/NEA benchmark exercise using a k-ϵ RANS turbulence closure are presented. The benchmark exercise consisted in simulating the mixing of a helium-rich mixture-air stable stratification initially at rest by a turbulent helium-air jet. The experiment depicted in Fig. 1 has been conducted in the PANDA facility ($\sim 90\,\mathrm{m}^3$) located at the Paul Scherrer Institute. A complete

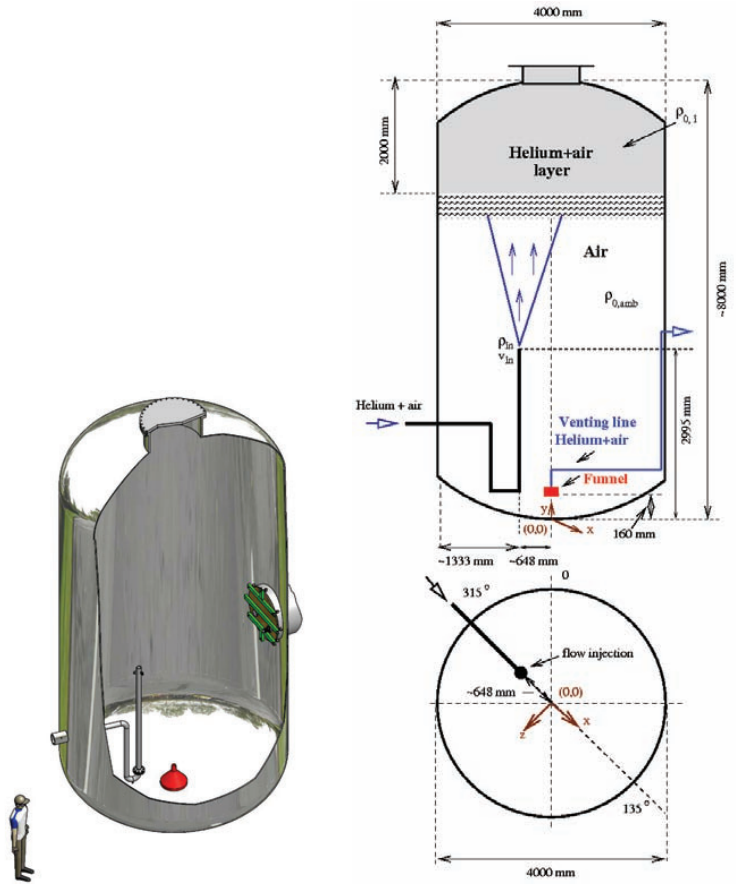

Figure 1: PANDA vessel and configuration used for the benchmark exercise

description of the benchmark specifications is beyond the scope of this paper and we refer the interested reader to [2] for a detailed description of the benchmark exercise.

Calculations have been carried out using the P^{2}REMICS (Partially PREMIxed Combustion Solver) computer code, developed by IRSN. This code is dedicated to the simulation of explosion related phenomena and includes the release and dispersion of explosive gases, explosion itself and the propagation of blast waves resulting from deflagration or detonation together with their interaction with surrounding structures.

P^{2}REMICS is based on the generic CFD solvers library CALIF^{3}S (Components Adaptative Library For Fluid Flow Simulations), itself built on the component library and programming environment PELICANS [1], which consists in a set of software component that can handle a wide range of applications. This includes laminar or turbulent flows, possibly reactive, governed by incompressible, low Mach number or compressible Navier-Stokes equations. Turbulence is treated either by using RANS modeling, mainly with one-point closure models following two-equation models with or without wall laws (low-Reynolds extension or elliptic relaxation), or by using LES.

The physical model used in P^{2}REMICS to compute the erosion of a stratified layer by a buoyant jet corresponds to the multi-species Navier-Stokes mixture model in the frame of the low Mach number approximation. This approximation is fully justified here as the Mach number does not exceed 0.01. Time discretization is performed by using a fractional step algorithm which consists in solving in sequence the set of balance equations (hydrodynamics, turbulence, ...). The hydrodynamic step is itself discretized in time using a fractional step scheme through a pressure correction method. Space discretization is performed by using a staggered finite volume scheme for which scalar unknowns (temperature, mass fractions, turbulent kinetic energy, ...) are located at cell centers while the velocity is located at cell faces. Convection operators use second order discretizations

(hybrid, MUSCL or QUICK) and diffusion operators are based on the usual second order differencing or on the more general version SUSHI (Scheme Using Stabilization and Hybrid Interfaces).

The simulations have been performed using a cartesian structured mesh as shown in Fig. 2. Since the cartesian structured mesh is particularly well suited to perform Large Eddy Simulations (LES) (*e.g* [7]), such a mesh has been retained here as we intend to perform LES and hybrid RANS-LES simulations and then to compare numerical results with those obtained in this work using RANS turbulence models. The meshing is stretched near walls and involves non-conforming local refinement in the spreading jet region and in the stratified region as illustrated in Fig. 2. The local refinement allows to get up to 16 cells in the injection diameter and this helps to impose the inlet velocity profile in accordance with the PIV data just above the pipe outlet.

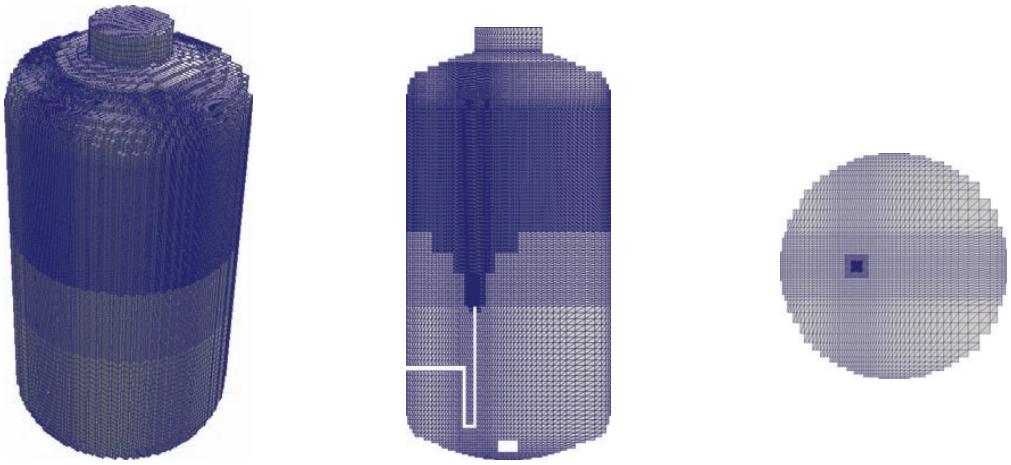

Figure 2: Meshing of the PANDA vessel. 3D view (left), z-y cutplane (center) showing the injection line and the funnel for the venting, z-x cutplane (right) corresponding to the injection elevation

The boundary conditions correspond to inlet conditions at the pipe outlet, inlet-outlet conditions at the funnel entrance and wall conditions on the vessel walls and the remaining of both the injection pipe and the funnel. The inlet conditions consist in imposing all the flow variables. The jet inflow velocity boundary condition is given by a hyperbolic tangent profile for the vertical component :

$$\frac{v(y)}{v_i} = \frac{1}{2} + \frac{1}{2}\tanh(\frac{r_0 - r}{2\delta}) \tag{5}$$

where $r = \sqrt{x^2 + z^2}$, r_0 is the pipe radius, $\delta = r_0/6$ is the initial momentum thickness of the annular shear layer and v_i is the injection velocity. The inlet turbulent kinetic energy k and turbulent dissipation ϵ are fixed following the common methodology, namely $k = 1.5(iv)^2$ and $\epsilon = C_\mu k^2/(r\nu)$ where i refers to the turbulent intensity and r is the ratio of the turbulent viscosity and the molecular viscosity. These have been fixed rather arbitrarily to the most commonly used values 0.1 and 25. respectively.

The governing transport equations for k and ϵ read :

$$\rho\frac{dk}{dt} = \nabla\cdot\left(\left(\mu + \frac{\mu_t}{\sigma_k}\right)\nabla k\right) + \mathcal{P}_k + \mathcal{P}_b - \rho\epsilon \tag{6}$$

$$\rho\frac{d\epsilon}{dt} = \nabla\cdot\left(\left(\mu + \frac{\mu_t}{\sigma_\epsilon}\right)\nabla \epsilon\right) + \frac{\epsilon}{k}\left(C_{\epsilon 1}\mathcal{P}_k + C_{\epsilon 3}\mathcal{P}_b - C_{\epsilon 2}\rho\epsilon\right) \tag{7}$$

where P_k and P_b denote the production of turbulent kinetic energy due to respectively the mean velocity gradients and buoyancy. Using the Simple Gradient Diffusion Hypothesis (SGDH) which represents the most common modeling approach, the buoyancy contribution term is given by:

$$P_b = -\frac{\mu_t}{\sigma_g}\frac{\nabla\rho}{\rho^2}\cdot(\nabla p + \rho_0\mathbf{g}) \tag{8}$$

Table I: k-ϵ model constants

C_μ	$C_{\epsilon 1}$	$C_{\epsilon 2}$	$C_{\epsilon 3}$	σ_k	σ_ϵ	σ_g
0.09	1.44	1.92	1.44	1	1.3	0.7

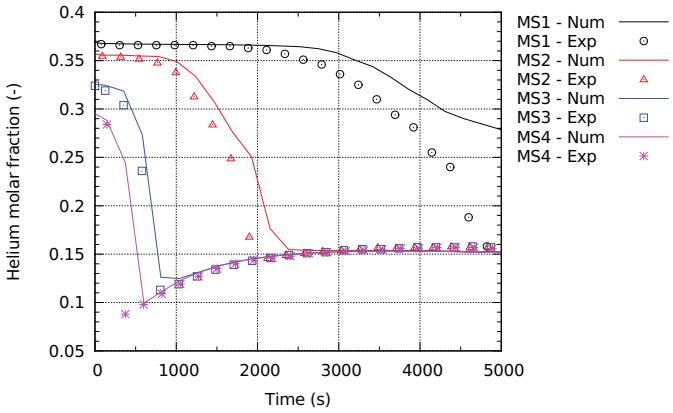

Figure 3: Time evolution of the helium molar fraction using the standard k-ϵ model and comparison with experimental data. MS1, MS2, MS3 and MS4 lie along the axis of injection and are located respectively at $y = 7.5$, 6.7, 6.2 and 6 m from the injection.

The coefficients C_μ, $C_{\epsilon 1}$, ... are listed in Table (I) and correspond to the standard k-ϵ model constants.
As the de-stratification process is the most important phenomenon adressed in the benchmark exercise, we first focus on the time evolution of the helium molar fraction. The comparison between the time evolution of the experimental helium molar fraction and that computed numerically is shown in Fig. 3. This figure which gather the sampling locations that lie along the axis of injection shows that the computed solution tends to under-predict the erosion process. Moreover, this discrepancy seems to grow up versus time when comparing for instance data coming from MS1 and MS2 sampling locations.

When comparing the mean velocity profiles at selected times as displayed in Fig. 4 and 5, one also observes some discrepancies between experimental and computed numerical data. While the first velocity profiles HVy1 shown in Fig. 5 located just above the pipe outlet are in good agreement with the PIV data, some discrepancies appear as one moves away from the pipe outlet. More specificaly, the spreading rate of the jet seems to be over-predicted leading to an underestimation of the mean centreline vertical velocity. This misestimation of the

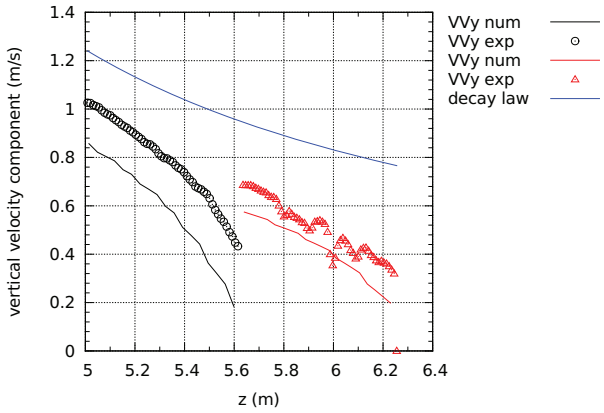

Figure 4: Mean vertical velocity component along the injection axis at selected times ($t = 111.\,\mathrm{s}$ for $5.0 \leq y \leq 5.6\,\mathrm{m}$ and $t = 1213.\,\mathrm{s}$ for $5.6 \leq y \leq 6.2\,\mathrm{m}$) and decay law according to Eq. 3

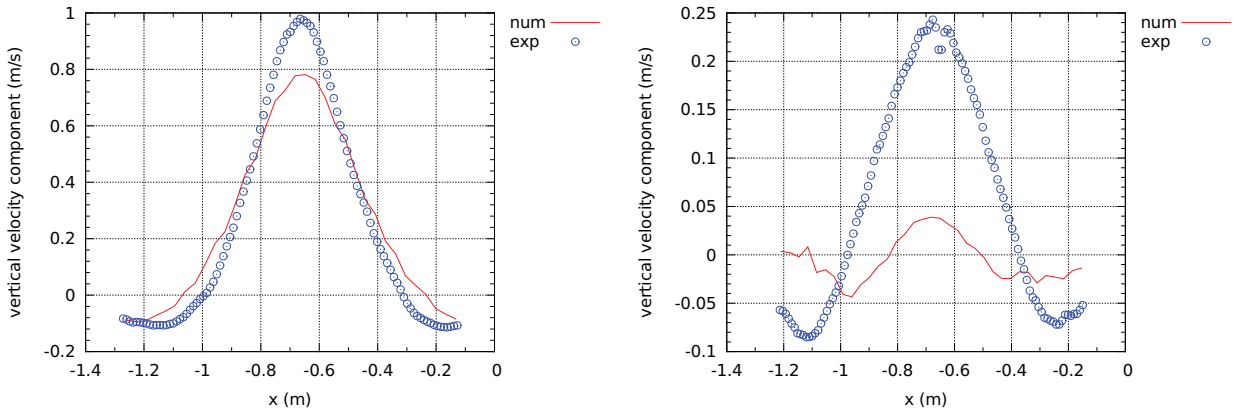

Figure 5: Mean vertical velocity component (HVy) along horizontal lines at $y = 5.1\,\mathrm{m}$ (left) and $y = 6.1\,\mathrm{m}$ (right)

spreading rate also participates to the misestimation of the erosion process illustrated in Fig. 3 as the impinging velocity at the stratified region is under-estimated. Other modeling limitations inherent to eddy diffusivity two-equation models directly affect the redirection of the jet and then the mixing process. The main limitations concern the well-known lack of universality of RANS models (model constants, modifications due to buoyancy, ...), the isotropy assumption used in eddy diffusivity models and the use of a single time scale to describe the turbulent motions. These limitations can be overcome, at least partially, by using more sophisticated turbulent models, typically Reynolds stress models to address the question of isotropy. However, as already pointed out in [18] and according to the some results presented at the benchmark exercise, benefits using more sophisticated RANS models (second moment closure) remain low compared to a turbulence modelling based on LES. The counterpart lies in the calculation cost that can be somewhat prohibitive for such large scale experiments and test duration. This calls to intermediate approaches, typically hybrid RANS-LES methods, that try to retain the highlights of both approaches.

4 SMALL-SCALE EXPERIMENTS AND HYBRID MODELS ASSESSMENT

The previous study indicates that small-scale experiments involving global and non-intrusive measurements would appear as a complementary and beneficial approach to investigate the observed discrepancies between RANS simulations and large-scale measurements. This would enable to investigate the different regions acting on the erosion process, as carried out in [18] but through numerical experiments, namely the variable density turbulent jet region, the impinging and the redirection region and also the role of the waves generated and transmitted in the upper part of the vessel. In this frame, small-scale experiments employing simulants fluids such as water-salt water pair appear as a good candidate as it allows to gain access to the different regions of interest using non-intrusive measurement techniques. Moreover, as the Schmidt number takes high values for such a fluid pair, this allows to focus on the turbulent mixing without considering additional molecular diffusion.

Before moving to selected small-scale experimental results, we first focuss on a continuous hybrid method ensuring a seamless transition between RANS and LES resolution. Among the proposed methods, we consider here as a first step the SAS (Scale-Adaptive Simulation) methodology [14, 13]. Starting from the transport equations for k and $\Phi = \sqrt{k}L$ proposed in [14], where $L = C_\mu^{3/4} k^{3/2}/\epsilon$ denotes the integral length scale, the

SAS version of the k-ϵ model reads [13] :

$$\rho\frac{dk}{dt} = \nabla\cdot\left(\left(\mu+\frac{\mu_t}{\sigma_k}\right)\nabla k\right)+\mathcal{P}_k+\mathcal{P}_b-\rho\epsilon-2\mu\frac{k}{d^2} \tag{9}$$

$$\begin{aligned}\rho\frac{d\epsilon}{dt} =& \nabla\cdot\left(\left(\mu+\frac{\mu_t}{\sigma_\epsilon}\right)\nabla\epsilon\right)-2\frac{\rho C_\mu}{\sigma_\epsilon}\epsilon^2\nabla\left(\frac{k}{\epsilon}\right)\cdot\nabla\left(\frac{k}{\epsilon}\right)\\ &+\frac{\epsilon}{k}\left(\mathcal{P}_k\left[C_{\epsilon1}+C_{\Phi2}\left(\frac{L}{L_v}\right)^2\right]+C_{\epsilon3}\mathcal{P}_b-C_{\epsilon2}\rho\epsilon\right)+\frac{\mu\epsilon}{d^2}\left(6f_\xi-4\right)\end{aligned} \tag{10}$$

where the last terms in the transport equations for k and ϵ correspond to additional low-Reynolds damping terms with f_ξ given by :

$$f_\xi=\frac{1+4.7\xi}{1+\xi^4}\,,\quad \xi=\frac{\rho\sqrt{0.3k}d}{20\mu} \tag{11}$$

where d denotes the distance from the nearest wall. The turbulent viscosity is expressed as usually as $\mu_t = \rho C_\mu k^2/\epsilon$. In comparison to the standard k-ϵ model, the SAS version contains two additional terms in the transport equation for ϵ. The first additional term corresponds to cross spatial derivatives for k and ϵ and comes from the transposition from the k-Φ model to the k-ϵ model. The second additional term is specific to the SAS methodology and involves the von Karman length scale defined as :

$$L_v=\kappa\left|\frac{u'}{u''}\right|\,,\quad u'=\sqrt{2s_{ij}s_{ij}}\,,\quad 2s_{ij}=\frac{\partial u_i}{\partial x_j}+\frac{\partial u_j}{\partial x_i}\,,\quad u''=\sqrt{\frac{\partial^2 u_i}{\partial x_j^2}\frac{\partial^2 u_i}{\partial x_k^2}} \tag{12}$$

where $\kappa = 0.41$ is the von Karman constant. Finally, the coefficient $C_{\Phi2}$ is determined from the logarithmic layer estimates and is given by :

$$C_{\Phi2}=\frac{\kappa^2}{\sigma_\epsilon\sqrt{C_\mu}}+C_{\epsilon2}-C_{\epsilon1} \tag{13}$$

The other model constants are reported in Table (II).

Table II: SAS k-ϵ model constants

C_μ	$C_{\epsilon1}$	$C_{\epsilon2}$	$C_{\epsilon3}$	σ_k	σ_ϵ	σ_g
0.09	1.2	1.83	1.2	2/3	2/3	0.7

Experiments are carried out in a plexiglass tank $0.5\,\mathrm{m}$ in height with a $0.3\,\mathrm{m}\times 0.3\,\mathrm{m}$ square cross-section. The tank is filled from the bottom up to a height h_2 of salt water, then from the height h_2 to h_1 of a water-salt water mixture with a linear density profile and, finally, from h_1 to $h_f = 0.45\,\mathrm{m}$ of water. The origin of the vertical z-axis was set to the upper plate of the facility and the z-axis is directed downwardly as illustrated in Fig. 6. The water is injected from a circular vertical nozzle $0.004\,\mathrm{m}$ in diameter, $0.06\,\mathrm{m}$ below the free surface and located at the center of the upper part. The injection is made by means of a pump that allows to fix the injection velocity to $1.33\pm0.15\,\mathrm{m.s^{-1}}$. As a result, the Reynolds number $\mathrm{Re}\simeq 5000$ still corresponds to a turbulent jet but is much smaller. This also means that LES appears to be tractable for such small-scale experiments as the disparity between the large scale structures and the dissipative ones is greatly reduced. The mean velocity and the rms kinetic energy have been measured by means of particle image velocimetry using a high-speed camera for the inside jet region and a slower one for the other regions. Small particles, about $10\,\mu$m in diameter, are used as seeding particles in the overall tank region whereas the jet is seeded with larger particles, about $250\,\mu$m in diameter, as it moves faster. As illustrated in Fig. 6, the PIV cameras are mounted in front of the tank, the laser sheet comes perpendicularly and pass through the jet axis. The density measurement technique is also based on a non-intrusive technique and corresponds to the synthetic schlieren technique.

As a preliminary study, experiments conducted on a inertial jet without stratification have been carried out in order to validate the PIV technique and to estimate the reliability of the turbulence modeling for such non-buoyant flow. We focus here on the mean vertical velocity along the z-axis for which numerous data have been produced. The results are displayed in Fig. 7 and are also compared with the usual decay law given by Eq.

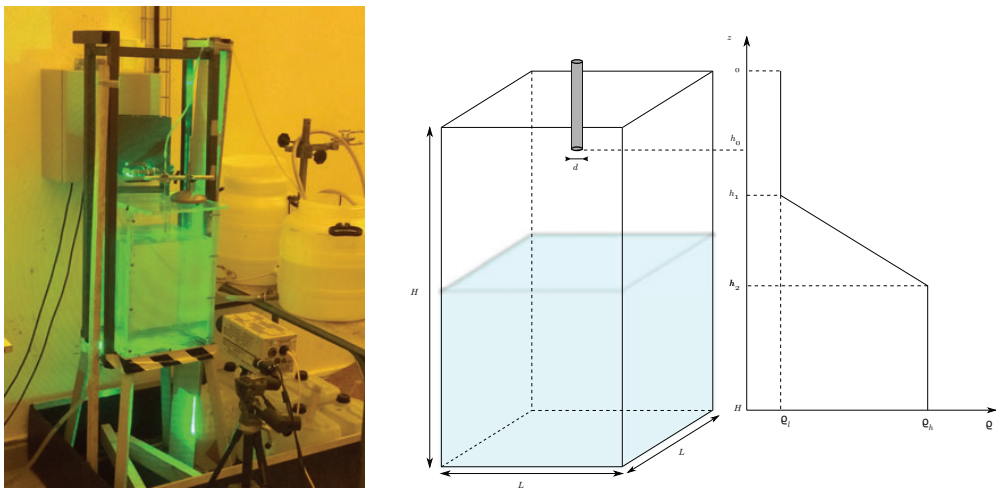

Figure 6: Picture (left) and sketch (right) of the small-scale experimental device

3. The reported decay constant from experimental measurements is found to be $B = 6.6$ which lies in the reported interval range 4.48-6.7. As expected, RANS simulations using the standard k-ϵ model predict a faster decay of the centreline axial mean velocity. One of the main reasons comes from the well-known plane/round jet anomaly [15]. On the other hand, SAS results are in a better agreement with experimental data and this confirms results obtained with the original SAS k-$\sqrt{k}L$ model [3, 14].

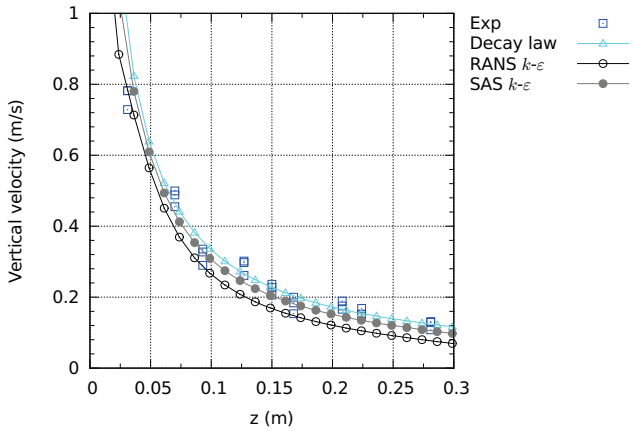

Figure 7: Axial decay of the mean centreline vertical velocity for the inertial jet without stratification (small-scale facility)

Work is currently in progress to study stratified situations. An example of the PIV measurements is reported in Fig. 8 corresponding to the regimes $\mathrm{Fr}_i \sim 1$ at two different times of the erosion process. As expected for this regime, the jet penetrates the stratified layer and is then redirected downwards with some secondary vortex structures. As the shape of the mean velocity structure and the rms fluctuating velocity govern the dynamic of the erosion process, these experimental results should allow to estimate the predictive capabilities of RANS turbulence models to compute this kind of variable density turbulent flow. A preliminary application of the SAS k-ϵ model is also provided in Fig. 9 which show a preliminary comparison between the results obtained for the density distribution from the RANS k-ϵ model, the SAS k-ϵ model and a LES calculation using the WALE subgrid viscosity model. This preliminary qualitative comparison clearly shows the potentialities of the SAS model as the results obtained on a coarse grid ($\sim$ 700000 cells) become closer to those obtained from LES simulations on a finer grid ($\sim$ 3000000 cells).

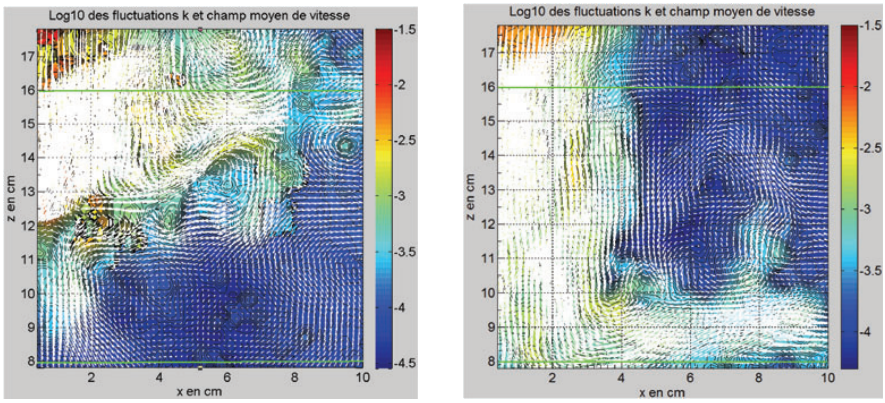

Figure 8: Velocity vector and turbulent kinetic energy during the erosion process corresponding to the regime $\mathrm{Fr}_i \sim 1$. Green lines correspond to the initial upper and lower boundary of the stratified layer

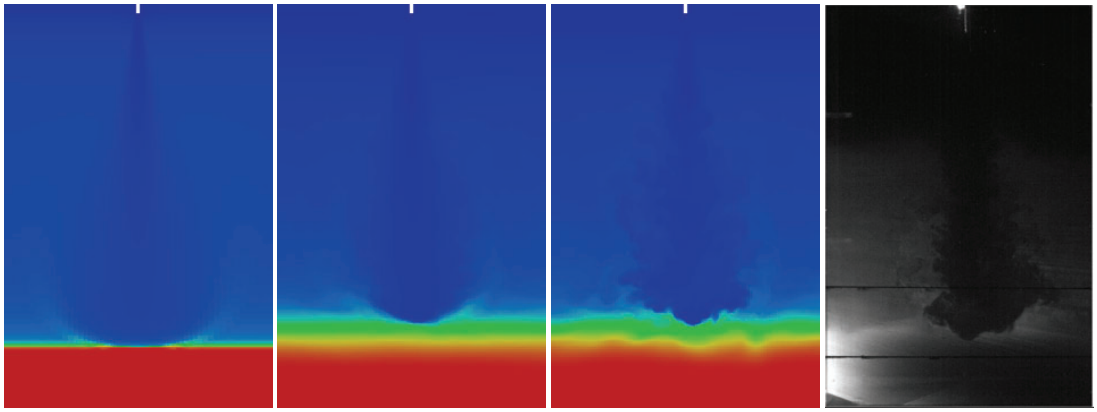

Figure 9: Snapshot of the density distribution - From left to right : RANS k-ϵ model, SAS k-ϵ model, LES WALE sgs model, experiments

5 CONCLUDING REMARKS

The aim of this paper was to assess the ability of hybrid RANS/LES methods to predict the mixing of a stable stratification. This evaluation has been carried out on calculations of the OECD/NEA-PSI benchmark exercise that concerns the erosion of a stratified layer by a buoyant jet. The results confirm the difficulty of RANS two-equation models to reproduce quantitatively such variable density turbulent flows. This probably comes from the inherent limitations of eddy diffusivity models (isotropy, single time scale, ...) and this argues for the use of LES approach. This was already pointed out from a purely numerical point of view [18] based on small-scale numerical experiments. Unfortunately, the use of LES appears to be somewhat prohibitive for such large-scale experiments and test duration. In this frame, development prospects based on small-scale experiments have been proposed. The interest of these small-scale experiments is twofold, it provides not only very detailed data regarding the flow structure by using non-intrusive measurements but also it provides the ability to perform LES calculations at a much lower cost. This allows to quantify the limits of RANS and LES approaches and to develop hybrid RANS-LES approach that appears to be a promising candidate for such kind of flow. A first qualitative comparison is provided in this paper that clearly shows the potentialities of the hybrid SAS approach.

REFERENCES

[1] PELICANS. Collaborative development environment. https://gforge.irsn.fr/gf/project/pelicans.

[2] OECD/NEA-PSI Benchmark specifications - Final version, 2014.

[3] K.S. Abdol-Hamid. Assessments of a turbulence model based on menter's modification to rotta's two-equation model. In *51st AIAA Aerospace Sciences Meeting including the New Horizons Forum and Aerospace Exposition*, number 2013-0341, 2013.

[4] M. Andreani, A. Badillo, and R. Kapulla. Synthesis of the OECD/NEA-PSI CFD benchmark exercise. In *CFD4NRS-5*, ETHZ, Zurich, Switzerland, 2014. OECD/NEA & IAEA Workshop.

[5] Michele Andreani, Ralf Kapulla, and Robert Zboray. Gas stratification break-up by a vertical jet: Simulations using the gothic code. *Nuclear Engineering and Design*, 249:71--81, aug 2012.

[6] C.G. Ball, H. Fellouah, and A. Pollard. The flow field in turbulent round free jets. *Progress in Aerospace Sciences*, 50:1--26, apr 2012.

[7] F. Boyer, F. Dardalhon, C. Lapuerta, and J.-C. Latché. Stability of a Crank-Nicolson pressure correction scheme based on staggered discretizations. *International Journal for Numerical Methods in Fluids*, 74(1):34--58, 2014.

[8] C. J. Chen and W. Rodi. *Vertical turbulent buoyant jets*. Number ISBN 0-08-024772-5. Pergamon press, 1980.

[9] Atabak Fadai-Ghotbi, Christophe Friess, Rémi Manceau, Thomas B. Gatski, and Jacques Borée. Temporal filtering: A consistent formalism for seamless hybrid RANS-LES modeling in inhomogeneous turbulence. *International Journal of Heat and Fluid Flow*, 31(3):378--389, jun 2010.

[10] Jochen Fröhlich and Dominic Von Terzi. Hybrid les/rans methods for the simulation of turbulent flows. *Progress in Aerospace Sciences*, 44(5):349--377, jul 2008.

[11] S. S. Girimaji and K. S. Abdol-Hamid. Partially-averaged Navier Stokes model for turbulence: Implementation and validation. In American Institute of Aeronautics and Astronautics, editors, *Aerospace Sciences Meeting and Exhibit*, volume 43rd. AIAA, 2005. AIAA 2005-502.

[12] J.M. Ma, S.-H. Peng, L. Davidson, and F.J. Wang. A low Reynolds number variant of partially-averaged Navier-Stokes model for turbulence. *International Journal of Heat and Fluid Flow*, 32(3):652--669, jun 2011.

[13] F.R. Menter and Y. Egorov. The scale-adaptive simulation method for unsteady turbulent flow predictions. part 1: Theory and model description. *Flow, Turbulence and Combustion*, 85:113--138, 2010.

[14] F.R. Menter, Y. Egorov, and D. Rusch. Steady and unsteady flow modelling using the k-$\sqrt{k}L$ model. In K. Hanjalic, Y. Nagano, and S. Jakirlic, editors, *Turbulence, Heat and Mass Transfer*, number 5, 2006.

[15] S. B. Pope. An explanation of the turbulent round-jet/plane-jet anomaly. *American Institute of Aeronautics and Astronautics Journal*, 16(3):279--281, 1978.

[16] R. Schiestel and A. Dejoan. Towards a new partially integrated transport model for coarse grid and unsteady turbulent flow simulations. *Theoretical and Computational Fluid Dynamics*, 18:443--468, 2005.

[17] E. Studer, J. Brinster, I. Tkatschenko, G. Mignot, D. Paladino, and M. Andreani. Interaction of a light gas stratified layer with an air jet coming from below: Large scale experiments and scaling issues. *Nuclear Engineering and Design*, 253:406--412, 2012. http://dx.doi.org/10.1016/j.nucengdes.2012.10.009.

[18] A. Zirkel. *Numerical investigation of the turbulence mass transport during the mixing of a stable stratification with a free jet*. PhD thesis, Stuttgart University, 2011.